49th AIAA Aerospace Sciences Meeting including the New Horizons Forum and Aerospace Exposition
4 - 7 January 2011, Orlando, Florida

AIAA 2011-1067

Refurbishment and Testing Techniques in a Transonic Ludwieg Tunnel

Thania S. Balcazar,* Eric M. Braun,† Frank K. Lu,‡ Duong Tran§ and Donald R. Wilson¶
University of Texas at Arlington, Arlington, Texas, 76019

Although cryogenic wind tunnels are typically used in industry for transonic testing, Ludwieg tunnels with high charge tube pressures can also produce unit Reynolds numbers high enough to match in-flight conditions. A brief timeline of transonic Ludwieg tunnel development is presented that shows how it was nearly selected for full-scale construction to compliment the National Transonic Facility. Having recently been refurbished, an overview of the unique high Reynolds number facility at UT Arlington is presented. Currently, experiments with the facility have been conducted using a combination of porous and solid walls with a half-span NACA 0012 model. Surface flow visualization techniques are discussed for this high Reynolds number, short duration facility. Future development efforts are presented to keep the facility suitable for current transonic testing topics.

Nomenclature

AOA	Angle of attack
M	Mach number
p_p	Plenum chamber static pressure
p_s	Test section static pressure
p_t	Charge tube stagnation pressure
SFV	Surface flow visualization
SSV	Sliding sleeve valve

I. Introduction

TRANSONIC wind tunnels must operate in a very high Reynolds number range in order to accurately replicate flight conditions for designing modern aircraft. The size of the test model and thus the size of the wind tunnel can be increased to directly increase the Reynolds number. Increasing density has a similar effect and was used for early wind tunnels.[1] As long as the specific heat ratio remains similar to air, an increase in the molecular weight of the test gas increases the density and decreases the velocity and viscosity. Decreasing the test gas temperature has the same effect, and the Reynolds number can be increased to several times its original value at a fixed pressure. Although all of these strategies have been applied in transonic tunnels, advances in technology have caused the cryogenic tunnel concept to develop and see widespread industrial use over the past thirty years.[2]

*Undergraduate Research Assistant, Aerodynamics Research Center, Department of Mechanical and Aerospace Engineering, Box 19018. Student Member.
†Graduate Research Associate, Aerodynamics Research Center, Department of Mechanical and Aerospace Engineering, Box 19018. Student Member.
‡Professor and Director, Aerodynamics Research Center, Department of Mechanical and Aerospace Engineering, Box 19018. Associate Fellow.
§Undergraduate Research Assistant, Aerodynamics Research Center, Department of Mechanical and Aerospace Engineering, Box 19018.
¶Professor, Aerodynamics Research Center, Department of Mechanical and Aerospace Engineering, Box 19018. Associate Fellow.

By 1965, supercritical airfoils capable of efficient operation at transonic speeds were successfully developed.[3] These airfoils led to the development of more maneuverable fighter aircraft like the F-111 that could operate at higher speeds.[4] The majority of wind tunnel testing and validation of these airfoils and aircraft was conducted in the NASA 8-foot transonic tunnel.[5] The 8-foot transonic tunnel design was the result of years of facility development that culminated with a slotted wall test section that could both eliminate interference from shock wave reflections and reach a freestream Mach number of about 1.2.[6] Despite these advances in testing capabilities, differences still existed between flight test results where direct comparisons were possible.[7] In his book, Goethert remarked that these differences may have been due to the fact that the Reynolds number of the wind tunnel models was below what occurred in flight.

In October of 1966, C-141 Starlifter flight test programs revealed a major shift in the center of pressure along the wings when the flight Mach number reached a range of 0.82–0.85.[8] Such behavior was not predicted with wind tunnel tests, and the flight speed had to be restricted while expensive and time-consuming improvements were made to the aircraft. By that time, a series of tests were conducted that showed shock-induced boundary layer separation was the main factor behind disagreement between wind tunnel and flight performance.[9] The location of the separation point, which is dependent on boundary layer thickness and thus the Reynolds number, can cause a large shift in the center of pressure. Once this scaling problem was recognized, studies were begun on how to design a wind tunnel capable of matching flight Reynolds numbers.[10] Other aircraft including the B-58, B-70, YF-12, F-102, and F-106 experienced unforeseen problems in transonic flight.[11]

Several competitive designs based on the methods discussed were developed in the late 1960s. A Ludwieg tube concept, first discussed in the 1950s,[12] was proposed to be combined with a high pressure charge tube. A preliminary design of such a tunnel consisted of an $8' \times 10'$ test section and a 770 psig stagnation pressure.[13] The overall length of the facility was slightly greater than one third of a mile and could produce a steady flow test time of a few seconds. It was compared with a blow-down tunnel of similar size and found to be more cost effective. Although the Ludwieg tube produces flow with very low turbulence, the major disadvantage of scaling it to such a size along with a 770 psig operating pressure is the forces produced on the test models. A $1/13^{\text{th}}$ scale model of this facility was built and characterized at the Arnold Engineering Development Center.[14,15] At the NASA Marshall Space Flight Center, construction of a larger transonic Ludwieg tunnel was completed in 1969.[16] A 32 inch, circular test section was connected to a 378 foot charge tube that could be pressurized to 700 psig and provided the highest unit Reynolds number of any western country at the time.[17] Development of a prototype transonic Ludwieg tube also progressed in Europe, where another large-scale facility was proposed for construction.[18] An AGARD FDP High Reynolds Wind Tunnel working group was formed in October 1969 that included members from the Netherlands, France, Germany, the United Kingdom, the United States, and Canada.[17] After subsequent meetings at the AEDC and MSFC facilities, designs for $16' \times 16'$ blowdown and $10' \times 10'$ Ludwieg tunnels were planned in detail.

Shortly thereafter, proof-of-concept tests were first conducted with the cryogenic tunnel concept at low-speeds.[19] The technology was then swiftly applied to a transonic tunnel. Engineering challenges with cryogenic tunnels included how to simultaneously inject a large quantity of liquid nitrogen and exhaust it in a gaseous phase, how to correctly insulate the tunnel, and how to ensure the overall tunnel structure would remain intact while exposed to such low temperatures.[2] Consequently, it appears the Ludwieg tunnel may have been the leading concept for large-scale development in 1970 until all of the challenges with cryogenic testing were addressed in the next couple years. In 1973, plans solidified to build both Ludwieg tube and cryogenic facilities to address specific needs for the Air Force and NASA. These plans were affected by the oil crisis and stock market crash of 1973 and 1974, which caused the cost estimate for the Ludwieg tunnel to more than double. After a series of compromises, the cryogenic tunnel was approved and construction began on the U.S. National Transonic Facility at NASA Langley.[11]

In November 1978, the University of Texas at Arlington acquired the $1/13^{\text{th}}$ scale Ludwieg tunnel after it was decommissioned from AEDC in 1976. At UT Arlington, the high Reynolds number capability was used for studying rotorcraft blade/vortex interactions[20,21] and advanced fighter wings.[22] Although the test model chord lengths are usually no more than 3 in., a Reynolds number of about 10 million/inch can be reached between Mach 0.5–1.2.[23] Considering the length of the test section, a flat plate arrangement could be constructed with a maximum Reynolds number of 250 million. Although the tunnel had fallen into disuse by 1999, it was refurbished in 2010 recognizing that it is a unique, low-cost facility that can have many uses for basic research. Perhaps the only comparable facility in operation at this time is the cryogenic Ludwieg tunnel at DLR Göttingen.[24]

II. Facility Characteristics

Ludwieg tube tunnels are based on using a fast-acting valve or diaphragm to open and generate an expansion wave to accelerate high-pressure air stored within a charge tube to a desired speed. If the tube is of constant area, then bursting a diaphragm on one end would simply cause an unsteady expansion wave to propagate into the tube at the speed of sound and reflect off the closed end. A nozzle can be added to control the flow speed in a test section after the wave passes by. A schematic of the facility at UT Arlington is shown in Fig. 1. The tunnel consists of a charge tube, convergent nozzle, test section, ejector flap section, diffuser, and starting sliding sleeve valve (SSV). High Reynolds numbers are obtained simply by filling the charge tube with high pressure air up to 45 atm.

The charge tube pressure in this facility directly relates to the desired test section Reynolds number. The expansion wave is generated by rapidly opening the SSV located at the end of the tunnel. As the wave travels through the charge tube, steady flow can theoretically be generated in the test section for 185 ms. However, the steady flow time is reduced to about 120 ms due to the time needed to open and reach a steady exhaust condition with the SSV. The charge tube is round, and a nozzle with a contraction ratio of 2.27 transitions to a rectangular test section measuring 7.28 in. (height), 9.14 in. (width), and 25 in. (length). Although the contraction ratio is fixed, the test section Mach number can be varied by keeping a certain portion of 27 ports open on the SSV to adjust the exhaust flow. The test section also utilizes porous walls to eliminate reflected shock waves. This allows test models of relatively large chord lengths to be used. Consequently, the test section is surrounded by a plenum chamber. The porous walls consist of two stacked plates with 60 deg inclined holes and a tapered porosity pattern in the upstream one third of the test section length. The thickness of the combined plates is 0.141 in. The holes in the wall are 0.120 in. apart on centers in both directions in the uniform porosity region. The porosity can be varied manually in the range from 3.5 to 10 percent by moving one plate relative to the other.

Implementing a test section with the porous walls required for transonic testing can be troublesome for a Ludwieg tube because air can travel through these walls into the test section from the plenum chamber as the expansion wave first travels by. Since Ludwieg tubes have relatively short run times, there is a possibility that steady flow may never be established before the expansion wave returns to the test section. Thus, an additional device is needed to ensure that the air in the test section flows out through the porous walls during the test. Figure 1 depicts two of eight tubes that lead from the plenum chamber to a section with a diaphragm holder. About 30 ms after the SSV is actuated, the diaphragm is cut, initiating another expansion wave traveling through the tubes towards the porous walls. If timed properly, the two expansion waves will merge and steady test section conditions are achieved. The plenum exhaust is also connected to a variable area ball valve which provides additional Mach number control. Ejector flaps mounted at the end of the test section provide a means for equilibrating it with the pressure in the plenum chamber, which can allow the Mach number to range from 0.5–1.2. The Reynolds number can be independently varied between 1–10 million/inch.

Instrumentation is located in the charge tube, plenum chamber, and test section. A thermocouple and

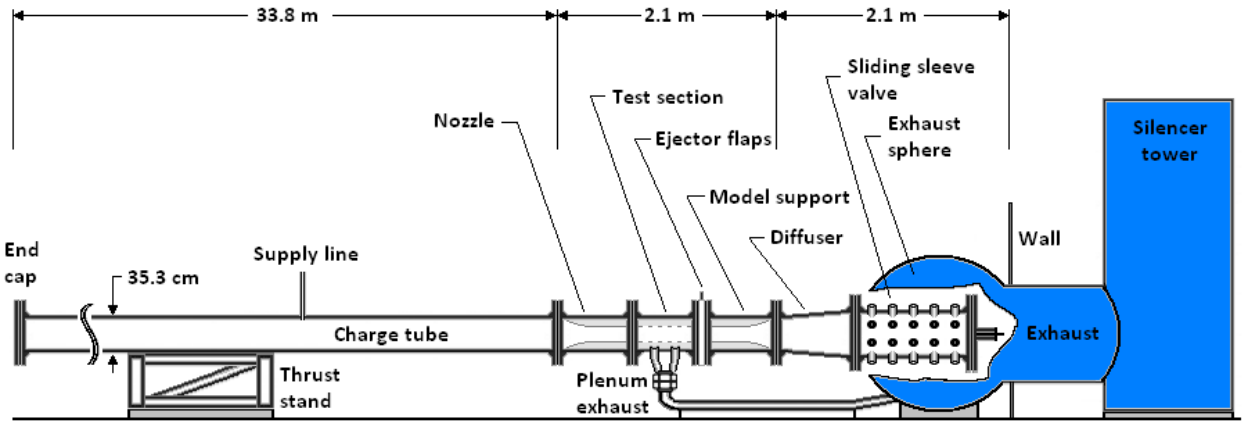

Figure 1. Elevation view of the UT Arlington HIRT Facility.

pitot probe are mounted along the wall of the charge tube to measure flow conditions prior to the nozzle. The total pressure measurement is used to calculate the Mach number in the rest of the tunnel sections. The Mach number is calculated from

$$M = \sqrt{\left(\frac{2}{\gamma - 1}\right)\left[\left(\frac{p_t}{p_s}\right)^{(\gamma-1)/\gamma} - 1\right]} \tag{1}$$

where p_s and p_t are the static and total pressure measured in the test section. Four static pressure ports are located in each side of the plenum chamber. A pressure measurement on each side can be used to indicate if the air is flowing uniformly through the porous walls, and all four can be utilized to estimate the test section Mach number using Eq. (1). As proven by centerline probe tests, the Mach number difference between the test section and plenum chamber flow is usually negligible. However, a difference can occur if the ejector flaps and porous walls are adjusted to settings that result in low mass removal.[25]

A. Test Section Configuration and Model

Instrumentation for the facility includes a Modern Machine & Tool 5-component sidewall force balance that fits into the test section through a 3-in. diameter optical port. When the balance was used previously, the porous sidewalls were removed and replaced with solid walls with a cutout for the balance. A plug is placed in the port opposite of the balance in order to preserve symmetry. Presumably, the top and bottom porous walls will dissipate reflections from any shocks stemming from the model mounted on the balance. For the

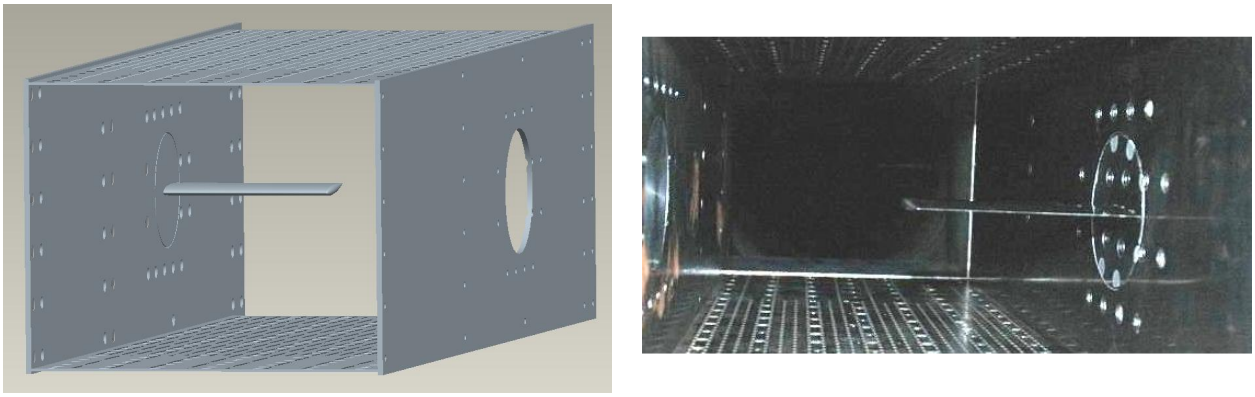

(a) Model of the wall configuration.

(b) Photograph of mounted airfoil.

Figure 2. Test section setup.

current study, a NACA 0012 model has been fit onto a disk with a diameter of slightly less than three inches which connects to the balance. The airfoil has a 2 in. chord & 4 in. span along with a rounded end that also follows the NACA 0012 profile. The force balance is free to rotate in the optical port before being tightened down, allowing for the angle of attack to be adjusted easily. The angle of attack is measured using a digital level and a reference surface attached to the balance. Due to the high force exerted on the model during the run, a small gap between the disk and the wall is required to allow the balance to flex without interfering with measurements. Force balance results are not presented in this study, but a dynamic calibration is planned since preliminary tests have shown a g-force present during the entire duration of the test. The raw voltage output from the normal force component channel was used to calibrate the reference surface to the true 0 degree angle of attack by finding the point where there was no lift.

B. Setup Validation

For this study, the setup has been validated at Mach 0.85 with a Reynolds number of about 1.5 million/inch. The ejector flaps were fully closed. Twelve sliding sleeve valve ports remain open to achieve this Mach number. The ball valve connected to the plenum cutter was set to nearly fully open in order to maximize mass removal from the porous walls. The ball valve acts as a fine tuning device for the Mach number since opening it along each of the 26 settings produces a ΔM of about 0.01. Figure 3(a) shows several pressure

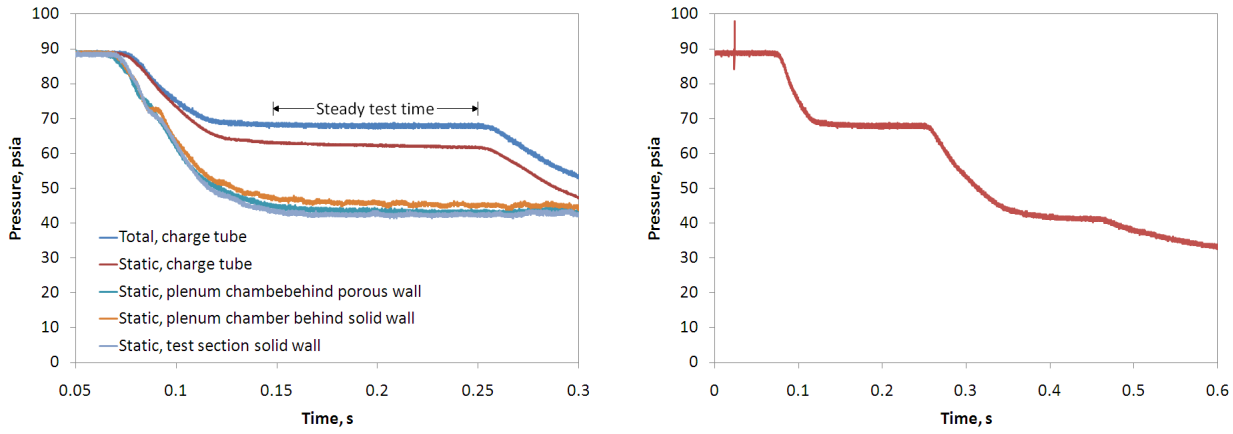

(a) Pressures during the test time.

(b) Charge tube stagnation pressure decay.

Figure 3. Pressure traces at a Mach 0.85 condition.

traces in the Ludwieg tunnel during the test. The total and static pressures in the charge tube indicate a Mach number of 0.34 during the test. Note that there is a slight difference in pressure between the static transducers in the plenum chamber behind the porous and solid walls. The test section static pressure as measured by a flush mounted transducer is nearly equal to the transducer behind the porous wall in the plenum chamber.

For a test time between 0.15–0.25 s in Fig. 3(a), the Mach number is 0.85 ± 0.015. Uncertainty was calculated with a 95 percent confidence interval. The Reynolds number is 1.7 million/inch. For this setup, performance appears to be reasonable when compared with previous pressure and Mach number data. Tests conducted at different Mach and Reynolds numbers have yielded similar results.

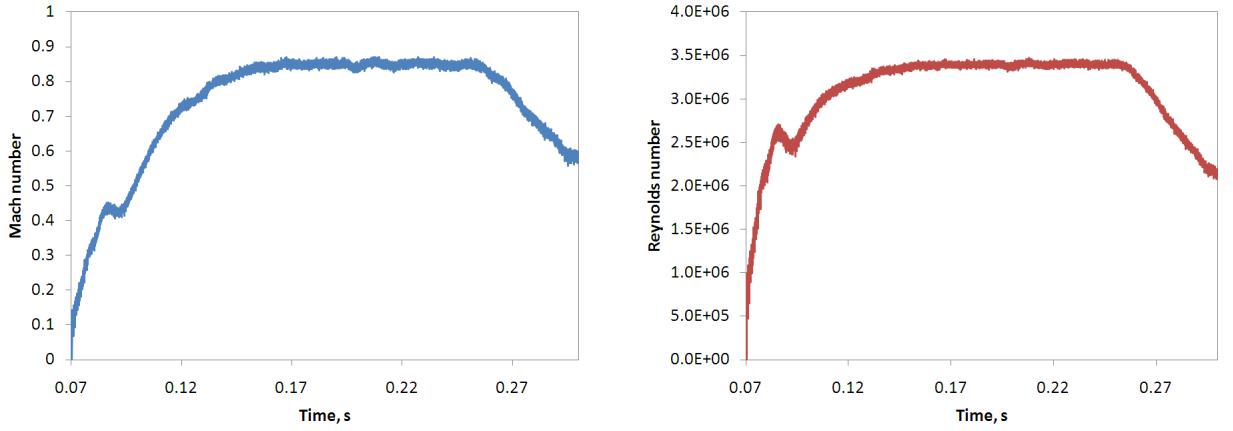

(a) Mach number.

(b) Reynolds number.

Figure 4. Typical performance at a Mach 0.85 condition.

III. SFV with Oil Flow Dots

Surface flow visualization using oil dots at different locations along the airfoil was considered for development with the Ludwieg tunnel due to its ability to reveal surface flow patterns.[26] This established method is often critiqued for the difficulty of distinguishing which of the oil mixture traces were made during the facility start-up process and which were made while running at the test conditions.[27] Occasionally, solid particles are added after the test conditions have been established, which is a difficult task with the Ludwieg

tunnel due to its short run time. The short start-up time before steady flow exists in the test section is assumed to cause minimal effects on the flow visualization.

The mixture consists of oil-based paint and SAE-85W140 gear oil. The paint/oil mixture ratio was about 2:3 for both colors chosen namely, blue and yellow. With precision in mind, the optimization of the application technique was a trial-and-error process. The most satisfactory application was done by using a soldering wire. Before each run, a row of blue dots followed by a row of yellow dots was placed at locations where features were evident in the fluorescent oil results as seen in Fig. 5(a).

In Fig. 5(d), the most evident features are the inward turning due to the pressure differences on the top and bottom of the airfoil. In addition, it is evident from the mixing of the blue and yellow traces that there is flow reversal closer to the trailing edge due to separation. Although separation can be identified at particular locations, the short run time disables the oil dot from making a complete trace along the entire airfoil, making it difficult to identify where the separation actually started. The shadow in the pictures is caused by the section attached to the airfoil. Besides flow reversal and inward turning, there are no other evident features in the results using this technique. A disadvantage of this technique is that it is mostly limited to visualizing only inward turning and separation. In Figs. 5(b) and 5(c), there is no significant difference in the oil-dot traces although the Mach numbers were different. Hence, the separation line, for example, would be very difficult to identify.

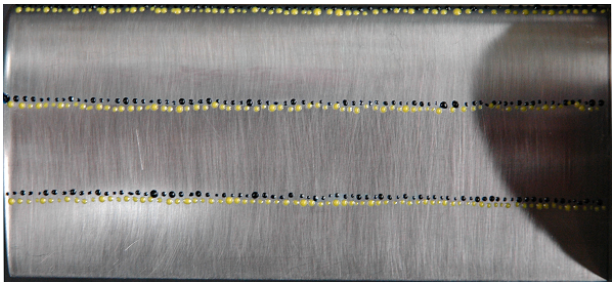

(a) Before a test.

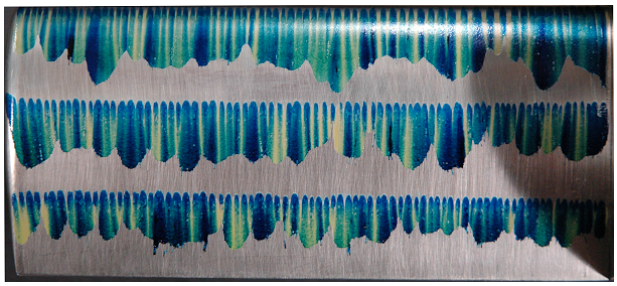

(b) 0 deg AOA test, Mach 0.685 $\pm$0.03, Re = 2.92×10^6.

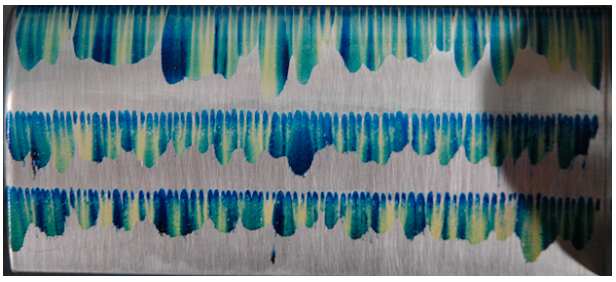

(c) 0 deg AOA test, Mach 0.85 $\pm$0.02, Re = 3.3×10^6.

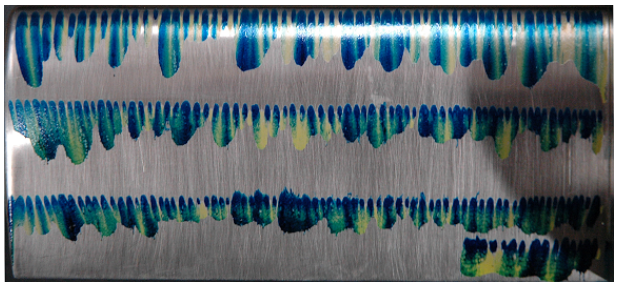

(d) 6 deg AOA test, Mach 0.85 $\pm$0.02, Re = 3.24×10^6.

Figure 5. SFV results with oil flow dots.

IV. SFV with Fluorescent Oil

Surface flow visualization along the airfoil with fluorescent pigment was considered for development with the Ludwieg tunnel due to its ability to reveal subtle features like the upstream influence[28] that should be present on the NACA 0012 airfoil for certain transonic conditions. Recent work by Pierce et al. with fluorescent chalk has been applied with the exception that a light oil is used as a carrier instead of kerosene and silicone.[29] In addition to its capability for producing high contrast images, the chalk produces small streaks along the surface that can indicate features of the flow.

This fluorescent mixture was applied with different consistencies in a trial-and-error process to reveal the flow pattern that should be present on the airfoil at Mach 0.85. Figure 6 shows two photographs of results that are rather poor. In Fig. 6(a), orange and blue bands were applied to the airfoil before the test. The blue chalk was ground to a fine powder using a 100 micrometer filter. Although it was ground, the orange chalk particles were much larger. Several of the orange bands show turbulence wedges developing

along the surface well before the same behavior is seen in the blue bands. Reviewing the work of Loving and Katzoff,[30] it appears the turbulent wedges are created by isolated rough spots from the orange particles. Both photographs also show the effects of having an oil coating that is too thick. When it is too thick or the mixture is too viscous, it does not flow well over the surface during the 100 ms test time. If it is applied only at the leading edge, it can give the false impression that the flow has separated.

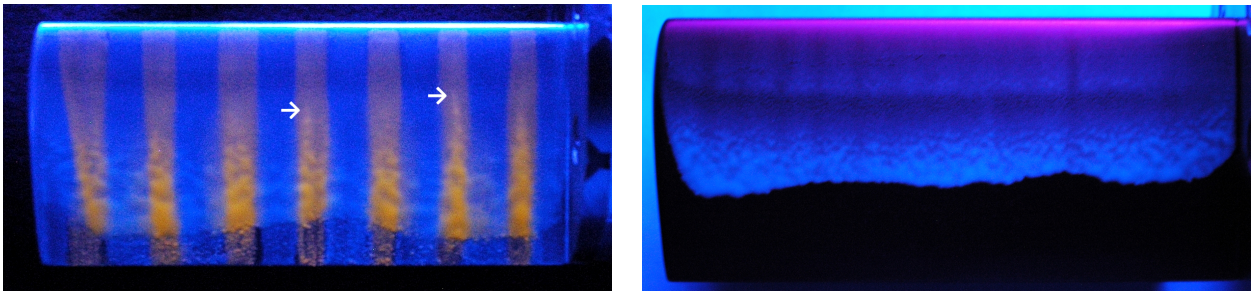

(a) Adverse effects of large fluorescent particles.

(b) Adverse effects with a viscous mixture that is heavily applied.

Figure 6. Fluorescent SFV tests with poor results.

To produce satisfactory results, the mixture was applied as a film with a soft brush over the entire surface of the airfoil prior to a test. Photographs taken for 0 and 6 degree AOA tests are shown along with sketches of the surface characteristics. For the 0 degree test, shock-induced boundary layer separation is clearly visible at an x/c location of about 0.6. At that point, the streaks left by the chalk particles are no longer visible and the surface appears blurred when compared to the rest of the airfoil. This location is similar to two-dimensional results obtained with $M = 0.84$–0.86 and Re = 3–4 million.[31,32] Several other features are visible. Near to the leading edge of the airfoil, transition appears to be marked with a line that is uniform across almost all of the airfoil. Transition causes a rise in shear stress, which affects the distribution of luminescent particles. After the transition point, a dark band appears around $x/c = 0.25$. This is visible for all fluorescent SFV experiments and could be related to weak waves over the airfoil. This could be a transient effect, and it appears too far upstream of the separation location to be related to the upstream influence. The upstream influence appears just before the separation and is more visible in the middle of the airfoil.

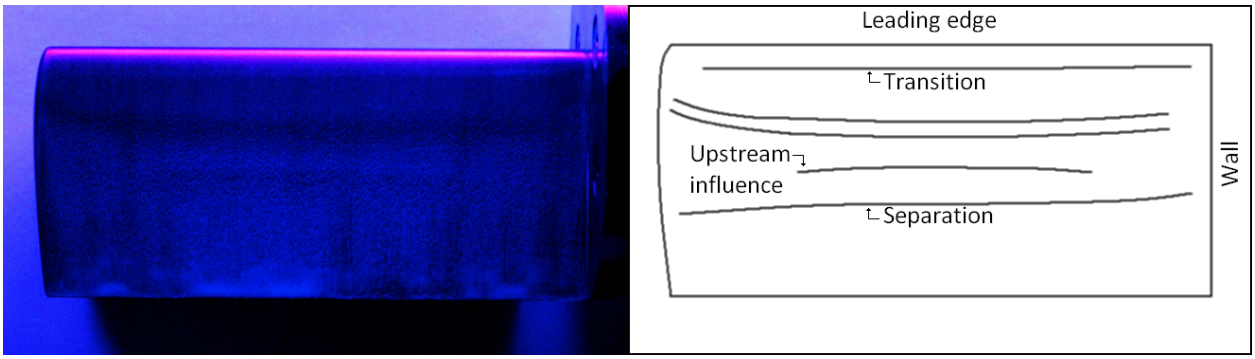

Figure 7. Fluorescent SFV of the airfoil at a 0 ± 0.2 degree AOA, Mach 0.85 ±0.015, and Re = 3.24×10^6.

Figure 8 shows a photograph and sketch of a Mach 0.87 test with the airfoil at a 6 degree AOA. Here, all of the surface flow characteristics move forward as anticipated. Inward turning that occurs due to the positive AOA is also visible in this case.

V. Conclusions

Although the studies presented here have been at a relatively low Reynolds number of 3 million, successful tests have been conducted with higher charge tube pressures. Future refurbishment work includes replacing

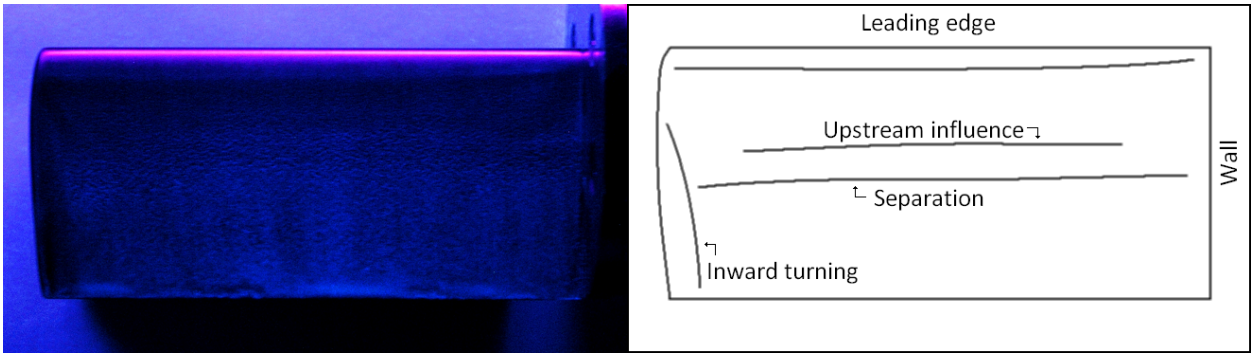

Figure 8. Fluorescent SFV of the airfoil at a 6 ± 0.2 degree AOA, Mach 0.87 ±0.025, and Re = 3.27×10^6.

and/or adding pneumatic lines to the air cylinder that drives the sliding sleeve valve since it tends to open slower for high charge tube pressures and causes more uncertainty in the pressure measurements during the test time.

The surface flow visualization techniques explored in this study were developed using a trial-and-error process from mixture content to application. Before these tests were conducted, it was unknown if useful results could be obtained due to effects from the initial expansion wave and its reflections. However, the location of shock-induced separation is evident from fluorescent SFV tests and it appears to match with similar experimental results. Further parametric studies using these SFV techniques will be performed at additional flow conditions.

The tunnel performs well using a combination of solid and porous walls. Uncertainty and pressure fluctuations may be further reduced by opening the ejector flaps in the future. Several additional test section combinations can be developed, especially since the complex porous wall slots can be manufactured more easily with equipment like a CNC waterjet. Since the SFV techniques should be able to indicate wall interference effects on the current model, perhaps porous slots can be arranged on a new semi-solid plate that can be implemented with the force balance. A flat plate can be added to the test section with optical access from the sides or top. A larger, two-dimensional airfoil model with static pressure ports could also be built that would fit though both optical ports. With several different test arrangements and techniques available, using this facility should be advantageous for fundamental research in the future.

Acknowledgments

The authors would like to thank Professor Joseph Schetz (Virginia Polytechnic Institute & State University) for the initial motivation and financial support to begin refurbishing the tunnel. Thania Balcazar was supported by a scholarship from the University of Texas at Arlington Undergraduate Research-based Achievement for STEM (AURAS). Duong Tran was supported by the University of Texas at Arlington "I Engage Mentoring Program."

References

[1]Munk, M. M. and Miller, E. W., "The Variable-density Wind Tunnel of the National Advisory Committee for Aeronautics," Tech. Rep. NACA TR-227, Langley Aeronautical Laboratory, Langley Field, VA, 1926.

[2]Kilgore, R. A., "Evolution and Development of Cryogenic Wind Tunnels," *43rd AIAA Aerospace Sciences Meeting*, Paper 2005-457, 2005.

[3]Whitcomb, R. T. and Clark, L. R., "An Airfoil Shape for Efficient Flight at Supercritical Mach Numbers," Tech. Rep. NASA TM X-1109, Langley Research Center, Langley Station, Hampton, VA, Jul. 1965.

[4]Ayers, T. G. and Hallissy, J. B., "Historical Background and Design Evolution of the Transonic Aircraft Technology Supercritical Wing," Tech. Rep. NASA TM-81356, NASA Dryden Flight Research Center, Edwards, CA, Aug. 1981.

[5]Wright, R. H., Ritchie, V. S., and Pearson, A. O., "Characteristics of the Langley 8-foot Transonic Tunnel with Slotted Test Section," Tech. Rep. NACA TR-1389, Langley Aeronautical Laboratory, Langley Field, VA, Jul. 1958.

[6]Goethert, B. H., *Transonic Wind Tunnel Testing*, Dover Publications, New York, 2007.

[7]Bird, K. D., "Model Configuration Tests in the C.A.L. 4 ft Transonic Tunnel: Correlation of Results from Different Scale Models over Wind Tunnels and Free Flight," Tech. rep., Arnold Engineering Development Center, Jul. 1956.

[8]Kraus, W. L., Matheson, J. M., Gustin, J., and Bryant, I. M., "C-141 Starlifter," Tech. rep., Office of MAC History, Scott AFB, IL, Jan. 1973.

[9]Loving, D. L., "Wind-tunnel–Flight Correlation of Shock-induced Separated Flow," Tech. Rep. NASA TN D-3580, Langley Research Center, Langley Station, Hampton, VA, Sep. 1966.

[10]Starr, R. F. and Schueler, C. J., "Experimental Studies of a Ludwieg Tube High Reynolds Number Transonic Tunnel," Tech. Rep. AEDC-TR-73-168, Arnold Engineering Development Center, Arnold AFB, TN, Dec. 1973.

[11]Jones, J. L., "The Transonic Reynolds Number Problem," *Workshop on High Reynolds Number Research*, NASA CP-2009, 1976.

[12]Ludwieg, H., "Tube Wind-Tunnel – A Special Type of Blowdown Tunnel," *AGARD-R-143*, Jul., 1957.

[13]Whitfield, J. D., Schueler, C. J., and Starr, R. F., "High Reynolds Number Transonic Wind Tunnels – Blowdown or Ludwieg Type?" *AGARD CP83*, Paper 29, Göttingen, Germany, April 26–28, 1971.

[14]Starr, R. F., "Experiments to Assess the Influence of Changes in the Tunnel Wall Boundary Layer on Transonic Wall Crossflow Characteristics," Tech. Rep. AEDC-TR-75-97, Arnold Engineering Development Center, Arnold AFB, TN, Nov. 1975.

[15]Sivells, J. C., "Calculation of the Boundary-layer Growth in a Ludwieg Tube," Tech. Rep. AEDC-TR-75-118, Arnold Engineering Development Center, Arnold AFB, TN, Dec. 1975.

[16]Warmbrod, J. D., "A Theoretical and Experimental Study of Unsteady Flow Processes in a Ludwieg Tube Wind Tunnel," Tech. Rep. NACA TN D-5469, George C. Marshall Space Flight Center, Marshall, AL, Nov. 1969.

[17]Anon., "Report of the High Reynolds Number Wind Tunnel Study Group of the Fluid Dynamics Panel," Tech. Rep. AGARD-AR-35-71, North Atlantic Treaty Organization, Apr. 1971.

[18]Ludwieg, H., Graner-Cartensen, H., and Lorenz-Meyer, W., "The Ludwieg Tube – A Proposal for a High Reynolds Number Transonic Wind-Tunnel," *AGARD-CP-174*, Paper 3, 1975.

[19]Goodyer, M. J. and Kilgore, R. A., "High-Reynolds-Number Cryogenic Wind Tunnel," *AIAA Journal*, Vol. 11, No. 5, 1973, pp. 613–619.

[20]Kalkhoran, I. M., Wilson, D. R., and Seath, D. D., "Experimental Investigation of the Perpendicular Rotor Blade-vortex Interaction at Transonic Speeds," *AIAA Journal*, Vol. 30, No. 3, 1992, pp. 747–755.

[21]Kalkhoran, I. M. and Wilson, D. R., "Experimental Investigation of the Parallel Rotor Blade-vortex Interaction at Transonic Speeds," *AIAA Journal*, Vol. 30, No. 8, 1992, pp. 2087–2092.

[22]Elbers, W. K., *Aerodynamic Investigation of Diamond Platforms*, Master's thesis, University of Texas at Arlington, Arlington, TX, 1991.

[23]Wilson, D. R. and Chou, S. Y., "Development of the UTA High Reynolds Number Transonic Wind Tunnel," *23rd AIAA Aerospace Sciences Meeting*, Paper 1985-315, 1985.

[24]Rosemann, H., Stanewsky, E., and Hefer, G., "The Cryogenic Ludwieg-Tube of DLR and its New Adaptive Wall Test Section," *26th AIAA Fluid Dynamics Conference*, Paper 1995-2198, 1995.

[25]Kalkhoran, I. M., *An Experimental Investigation of the Perpendicular Vortex-Airfoil Interaction at Transonic Speeds*, Doctoral dissertation, University of Texas at Arlington, Arlington, TX, 1987.

[26]Merzkirch, W., *Flow Visualization*, Academic Press, Inc., Orlando, 1987.

[27]Lepicovsky, J., "Investigation of Flow Separation in a Transonic-fan Linear Cascade Using Visualization Methods," *Experiments in Fluids*, Vol. 44, No. 6, 2008, pp. 939–949.

[28]Lu, F. K., "Surface Oil Flow Visualization: Still Useful After All These Years," *European Physical Journal – Special Topics*, Vol. 182, 2010, pp. 51–63.

[29]Pierce, A. J., Lu, F. K., Bryant, D. S., and Shih, Y., "New Developments in Surface Oil Flow Visualization," *27th AIAA Aerodynamic Measurement Technology and Ground Testing Conference*, Paper 2010-4353, 2010.

[30]Loving, D. L. and Katzoff, S., "The Fluorescent Oil-Film Method and Other Techniques for Boundary-Layer Flow Visualization," Tech. Rep. NASA MEMO 3-17-59L, Langley Research Center, Langley Field, VA, Mar. 1959.

[31]Harris, C. D., "Two-Dimensional Aerodynamic Characteristics of the NACA 0012 Airfoil in the Langley 8-Foot Transonic Pressure Tunnel," Tech. Rep. NASA TM-81927, Langley Research Center, Hampton, VA, Apr. 1981.

[32]Mineck, R. E. and Hartwich, P. M., "Effect of Full-Chord Porosity on Aerodynamic Characteristics of the NACA 0012 Airfoil," Tech. Rep. NASA TP-3591, Langley Research Center, Hampton, VA, Apr. 1996.